

## Different Regions in Skeletal and Cardiac Muscle Ryanodine Receptors Are Involved in Transducing the Functional Effects of Calmodulin\*

Received for publication, May 25, 2004, and in revised form, June 22, 2004  
Published, JBC Papers in Press, June 23, 2004, DOI 10.1074/jbc.M405834200

Naohiro Yamaguchi, Le Xu, Kelly E. Evans, Daniel A. Pasek, and Gerhard Meissner‡

From the Department of Biochemistry and Biophysics, University of North Carolina, Chapel Hill, North Carolina 27599-7260

Calmodulin (CaM) inhibits the skeletal muscle ryanodine receptor-1 (RyR1) and cardiac muscle RyR2 at micromolar  $\text{Ca}^{2+}$  but activates RyR1 and inhibits RyR2 at submicromolar  $\text{Ca}^{2+}$  by binding to a single, highly conserved CaM-binding site. To identify regions responsible for the differential regulation of RyR1 and RyR2 by CaM, we generated chimeras encompassing and flanking the CaM-binding domain. We found that the exchange of the N- and C-terminal flanking regions differentially affected RyR1 and RyR2. A RyR1/RyR2 chimera with an N-terminal flanking RyR2 substitution (RyR2 amino acid (aa) 3537–3579) was activated by CaM in single channel measurements at both submicromolar and micromolar  $\text{Ca}^{2+}$ . A RyR2/RyR1 chimera with a C-terminal flanking the 86-amino acid RyR1 substitution (RyR1 aa 3640–3725) bound  $^{35}\text{S}$ -CaM but was not inhibited by CaM at submicromolar  $\text{Ca}^{2+}$ . In this region, five non-conserved amino acid residues (RyR1 aa 3680 and 3682–3685 and RyR2 aa 3647 and 3649–3652) differentially affect RyR helical probability. Substitution of the five amino acid residues in RyR1 with those of RyR2 showed responses to CaM comparable with wild type RyR1. In contrast, substitution of the five amino acid residues in RyR2 with those of RyR1 showed loss of CaM inhibition, whereas substitution of the five RyR2 sequence residues in the RyR2 chimera containing the RyR1 calmodulin-binding domain and C-flanking sequence restored wild type RyR2 inhibition by CaM at submicromolar  $\text{Ca}^{2+}$ . The results suggest that different regions are involved in CaM modulation of RyR1 and RyR2. They further suggest that five non-conserved amino acids in the C-terminal region flanking the CaM-binding domain have a key role in CaM inhibition of RyR2.

$\text{Ca}^{2+}$ -release channels, known as ryanodine receptors (RyR),<sup>1</sup> play a key role in a variety of cells by increasing the cytoplasmic  $\text{Ca}^{2+}$  concentration in response to cellular signals. Three different RyR genes have been identified in mammalian cells: skeletal type (*RyR1*), cardiac type (*RyR2*), and brain type (*RyR3*) (1–3). The RyRs form large protein complexes composed

of four 565-kDa subunits and four small FK506-binding proteins. Multiple small physiological molecules such as  $\text{Ca}^{2+}$ ,  $\text{Mg}^{2+}$ , and ATP and proteins such as protein kinases and calmodulin (CaM) modulate RyR ion channel function (1–3).

CaM is a small cytosolic  $\text{Ca}^{2+}$ -binding protein that regulates various cellular functions (4, 5). Direct CaM binding inhibits all three RyR isoforms at  $[\text{Ca}^{2+}] > 1 \mu\text{M}$ , whereas at  $[\text{Ca}^{2+}] < 1 \mu\text{M}$  RyR1 and RyR3 are activated, but RyR2 is inhibited by CaM (6, 7).  $^{35}\text{S}$ -CaM binding to sarcoplasmic reticulum vesicles (8, 9) and purified RyR1 and RyR2 (10) showed that the two receptor isoforms bind one molecule of CaM per RyR subunit in the absence and presence of  $\text{Ca}^{2+}$ . CaM protection of trypsin digestion of RyR1 (11) and site-directed mutagenesis of RyR1 (12) and RyR2 (13) demonstrated that the two RyRs have a single CaM regulatory binding domain (CaMBD) (aa 3614–3643 in RyR1) for the  $\text{Ca}^{2+}$ -free and  $\text{Ca}^{2+}$ -bound ( $\text{Ca}^{2+}$ -CaM) forms of CaM. The CaM-binding domain is highly conserved among the mammalian isoforms, yet corresponding mutations in the RyR1 and RyR2 CaM-binding domain resulted in a different response to CaM in  $^{35}\text{S}$ -CaM binding and functional measurements (13). This result suggests that other isoform-specific regions are responsible for the differential modulation of RyR1 and RyR2 by CaM.

To test the hypothesis of an involvement of isoform-specific regions in regulating RyR1 and RyR2 by CaM, we constructed a series of RyR1/RyR2 chimeras and determined their CaM-binding properties and modulation by CaM. The results suggest that multiple regions are involved in transducing the functional effects of CaM in RyR1 and RyR2. The present study focused on the role of one of these regions. We found that substitution of five amino acid residues in RyR2 with those of RyR1 eliminated CaM inhibition but not CaM binding at  $[\text{Ca}^{2+}] < 1 \mu\text{M}$ .

### EXPERIMENTAL PROCEDURES

**Materials**— $^{3}\text{H}$ Ryanodine was obtained from PerkinElmer Life Sciences, Tran $^{35}\text{S}$ -label from ICN Radiochemicals (Costa Mesa, CA), unlabeled ryanodine from Calbiochem, Complete protease inhibitors from Roche Applied Science, and HEK293 cells from the American Type Culture Collection. RyR2 cDNA was kindly provided by Dr. Junichi Nakai of RIKEN Brain Science Institute (Wako, Japan). Unlabeled CaM and  $^{35}\text{S}$ -CaM were prepared as described previously (10).

**Construction of RyR cDNAs**—The full-length rabbit RyR1 (14) and RyR2 (15) cDNAs were subcloned into expression vectors pCMV5 and pCIneo, respectively. Single and multiple base changes were introduced by *Pfu*-turbo polymerase-based chain reaction, using mutagenic oligonucleotides and the QuikChange site-directed mutagenesis kit (Stratagene, La Jolla, CA). The complete mutated DNA fragments amplified by PCR were confirmed by DNA sequencing. A schematic summary and the amino acid numbers of RyR chimeras are shown in Fig. 1.

To construct RyR2-based chimeras and mutants, a ClaI/SacII-(10483–11203) fragment of RyR2 was subcloned into pBluescript KS vector. For RyR1-based chimeras and mutants (except RyR1-10M), an EclXI/NdeI-(10741–11173) (for 1-2-1, 1-2-1(C), and RyR1-5M) or an

\* This work was supported by National Institutes of Health Grants HL 73051 and AR18687. The costs of publication of this article were defrayed in part by the payment of page charges. This article must therefore be hereby marked “advertisement” in accordance with 18 U.S.C. Section 1734 solely to indicate this fact.

‡ To whom correspondence should be addressed. Tel.: 919-966-5021; Fax: 919-966-2852. E-mail: meissner@med.unc.edu.

<sup>1</sup> The abbreviations used are: RyR, ryanodine receptor; CaM, calmodulin; CaMBD, CaM-binding domain; WT, wild type; aa, amino acid; M, mutant; rev, reverse (mutation); Pipes, 1,4-piperazinediethanesulfonic acid.

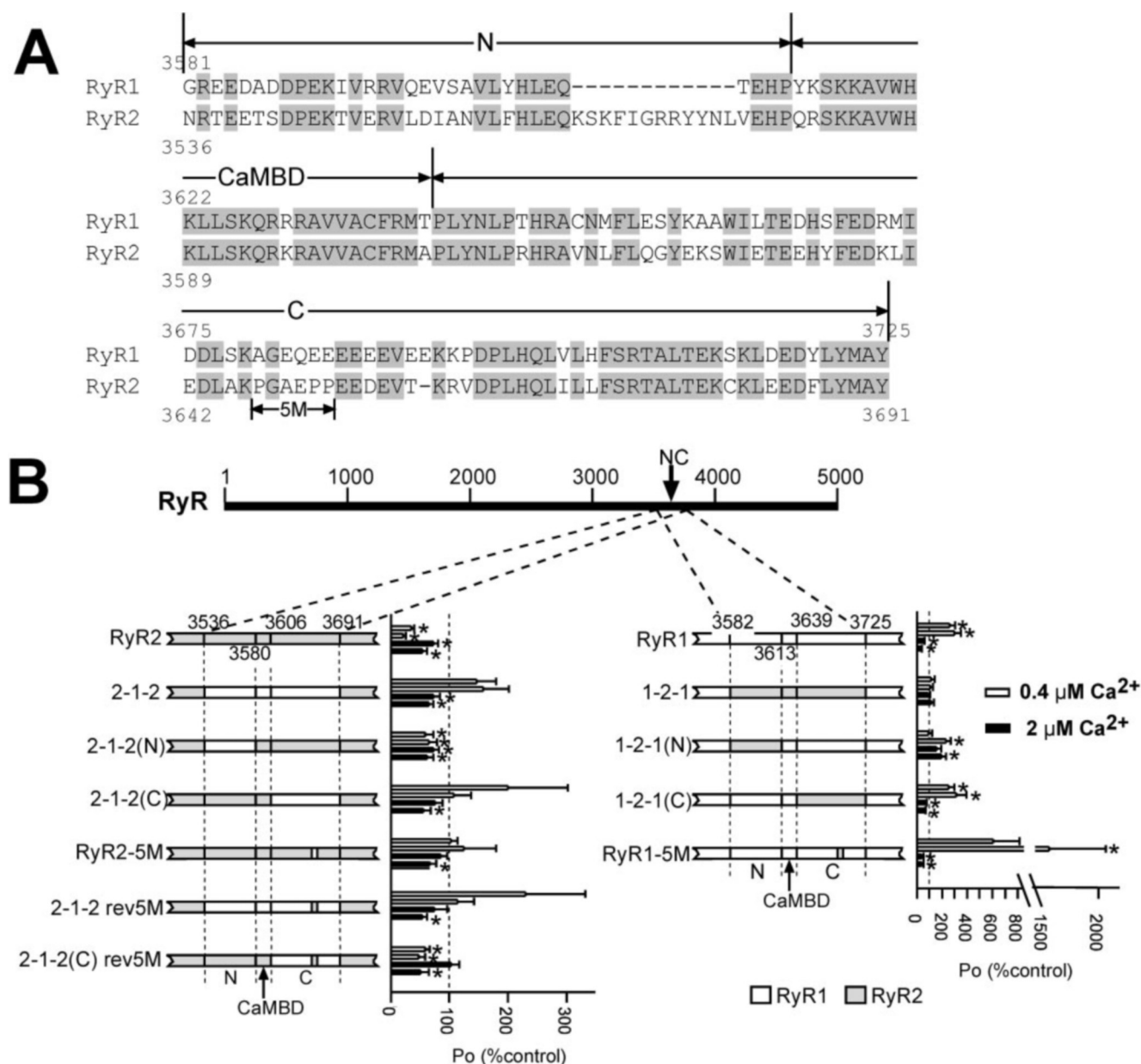


**FIG. 1. Sequence alignment of RyR1 and RyR2 chimeras and their modulation by calmodulin at 0.4 and 2  $\mu\text{M}$   $\text{Ca}^{2+}$ .** A, sequences of rabbit RyR1 (16) and RyR2 (15) CaMBD and N- and C-terminal flanking regions are shown. Chimeras 1-2-1 and 1-2-1(N) contain a 43-amino acid RyR2 substitution (aa 3537–3579), whereas chimeras 2-1-2 and 2-1-2(N) contain a 32-amino acid RyR1 substitution (aa 3581–3612). 5M, mutated region in RyR1-5M and RyR2-5M; N and C, substituted regions in RyR1/RyR2 chimeras. B, schematic representation of RyR1-based (right panel) and RyR2-based (left panel) chimeras and mutants and their modulation by CaM. Open bars, RyR1 sequences; shaded bars, RyR2 sequences. Channel open probabilities are shown on the right of panels. Data show the relative mean channel open probability ( $P_{o-\text{CaM}} = 100\% \pm \text{S.E.}$  of 4–15 single channel recordings at 0.4  $\mu\text{M}$   $\text{Ca}^{2+}$  plus 1 mM ATP (RyR1 only) (open bars) and 2  $\mu\text{M}$   $\text{Ca}^{2+}$  (filled bars) in the presence of 50 nM (upper open and filled bars) and 1  $\mu\text{M}$  (lower open and filled bars) CaM. \*,  $p < 0.05$  compared with control (-CaM).

EclXI/BamHI-(10741–10983) (for 1-2-1(N)) fragment was subcloned into pBluescript KS vector. The creation of 1-2-1 and 2-1-2 chimeras involved the use of a common restriction enzyme site (NdeI, 11173 of RyR1, and 11071 of RyR2) and the introduction of a new site (EclXI) in RyR2 at a location corresponding to the EclXI site in RyR1. For other chimeras, additional specific enzyme sites (SphI for 1-2-1(N) and 2-1-2(N) and NcoI for 1-2-1(C) and 2-1-2(C)) were introduced at corresponding positions in the RyR1 and RyR2 sequences. The aforementioned EclXI site was also used for obtaining 1-2-1(N) and 2-1-2(N), and EclXI/SphI and NcoI/NdeI fragments were exchanged for N- and C-terminal replacements, respectively. After construction of the chimeric fragments, sequences of SphI and NcoI sites were changed back to the original sequences in order not to cause amino acid changes.

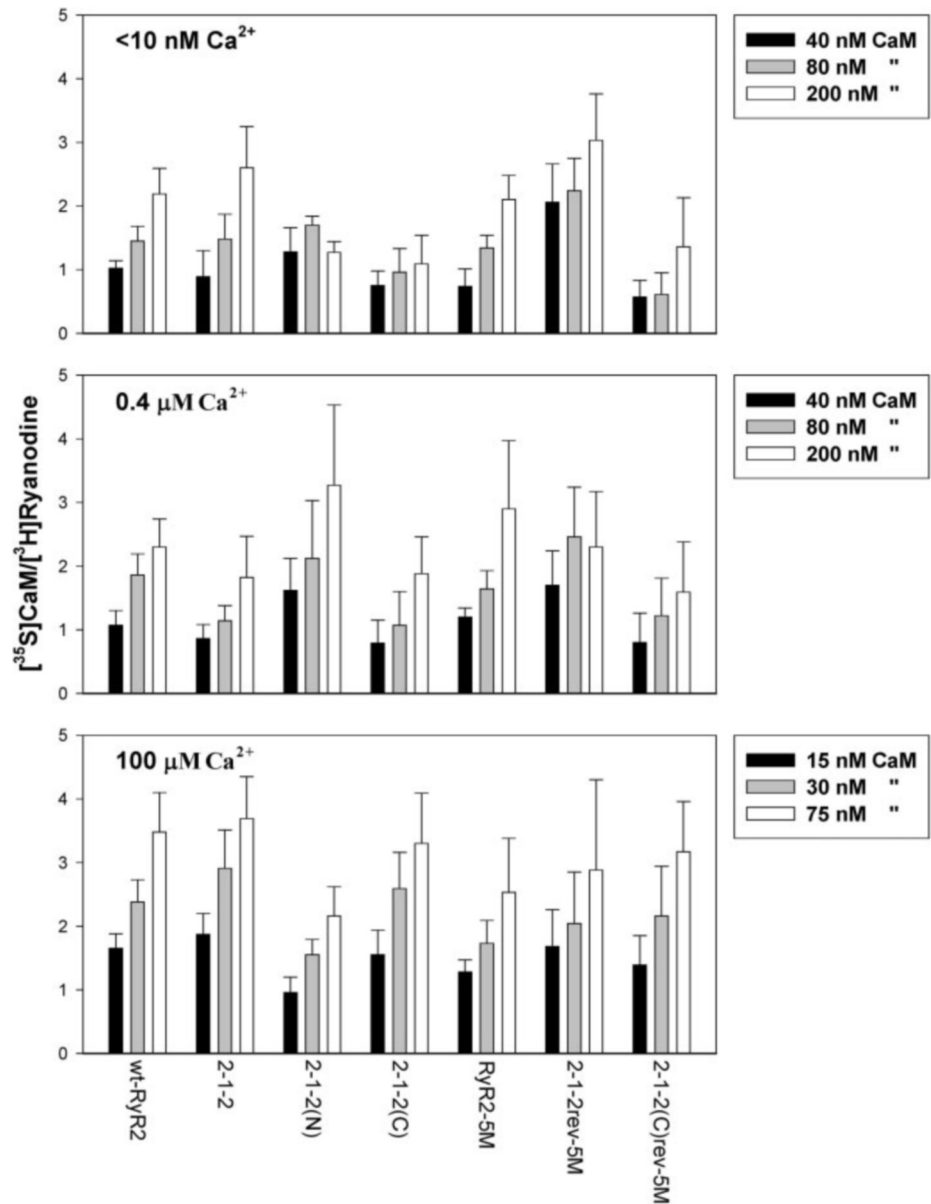
The chimeric ClaI/SacII fragment was subcloned back to the original position of a vector containing the BbrPI/SacII-(5038–11203) fragment of RyR2 and then to full-length RyR2 in the pCIneo expression vector to construct the full-length RyR2-based chimera expression plasmids. The

chimera EclXI/NdeI or EclXI/BamHI fragment was subcloned back to a vector containing a PvuI/NdeI-(8469–11173) fragment of RyR1 and then to a vector containing PvuI/XbaI-(8469-polylinker) fragment. Full-length expression plasmids for RyR1-based chimeras were prepared by ligation of two fragments (ClaI/PvuI and PvuI/XbaI) and expression vector pCMV5 (ClaI/XbaI).

To construct RyR1-10M, a vector containing the PinAI/XhoI-(4935–6467) fragment of RyR1 was used as a template for mutagenesis. The mutated fragment was subcloned back to a vector containing ClaI/PvuI-(polylinker-8469), and then a full-length expression plasmid was prepared by 3' fragment ligation as described above. Nucleotide numbering is as described previously (15, 16).

**Expression of Full-length RyRs in HEK293 Cells**—RyR cDNAs were transiently expressed in HEK293 cells with FuGENE 6 (Roche Applied Science) according to the manufacturer's instruction. Cells were maintained at 37  $^{\circ}\text{C}$  and 5%  $\text{CO}_2$  in high glucose Dulbecco's modified Eagle's medium containing 10% fetal bovine serum and were plated the day

FIG. 2.  $^{35}\text{S}$ -CaM binding to WT-RyR2, RyR2-based chimeras, and mutants. Membrane fractions prepared from HEK293 cells expressing WT-RyR2, RyR2 chimeras, and mutants were incubated for 2.5 h at room temperature with indicated concentrations of  $^{35}\text{S}$ -CaM in the presence of  $<10\text{ nM Ca}^{2+}$  (top),  $0.4\text{ }\mu\text{M Ca}^{2+}$  (middle), and  $100\text{ }\mu\text{M Ca}^{2+}$  (bottom). The ratios of  $^{35}\text{S}$ -CaM binding values to maximal binding values of [ $^3\text{H}$ ]ryanodine were obtained, taking into account that there is one high affinity [ $^3\text{H}$ ]ryanodine-binding site per RyR2 tetramer. Data are the mean  $\pm$  S.E. of 3–13 experiments.



before transfection. For each 10-cm tissue culture dish,  $3.5\text{ }\mu\text{g}$  of cDNA was used. Cells were harvested 48 h after transfection, and crude membrane fractions were prepared as described previously (12).

**$^{35}\text{S}$ -Calmodulin Binding**—Crude membrane fractions of HEK293 cells were incubated for 2.5 h at room temperature with  $15\text{--}200\text{ nM }^{35}\text{S}$ -CaM in  $20\text{ mM}$  imidazole,  $\text{pH } 7.0$ ,  $0.15\text{ M}$  sucrose,  $150\text{ mM}$  KCl,  $0.1\text{ mg/ml}$  bovine serum albumin,  $5\text{ mM}$  glutathione (reduced),  $25\text{ }\mu\text{M}$  leupeptin,  $250\text{ }\mu\text{M}$  Pefabloc, and either  $5\text{ mM}$  EGTA,  $0.4\text{ }\mu\text{M Ca}^{2+}$ , or  $100\text{ }\mu\text{M Ca}^{2+}$ . Aliquots were taken for determination of total radioactivity and centrifuged for 30 min at  $90,000 \times g$  in a Beckman Airfuge to obtain bound  $^{35}\text{S}$ -CaM. Radioactivity levels were determined by scintillation counting. Nonspecific binding of  $^{35}\text{S}$ -CaM was determined by incubating equal amounts of protein derived from vector-transfected HEK293 cells.

In parallel experiments,  $B_{\text{max}}$  values of [ $^3\text{H}$ ]ryanodine binding were determined by incubating membranes at room temperature with a saturating concentration of [ $^3\text{H}$ ]ryanodine ( $40\text{ nM}$ ) in  $20\text{ mM}$  imidazole,  $\text{pH } 7.0$ ,  $0.6\text{ M}$  KCl,  $0.15\text{ M}$  sucrose,  $25\text{ }\mu\text{M}$  leupeptin,  $250\text{ }\mu\text{M}$  Pefabloc, and  $200\text{ }\mu\text{M Ca}^{2+}$ . Nonspecific binding was determined using a 1000–2000-fold excess of unlabeled ryanodine. After 5 h, samples were diluted with 8 volumes of ice-cold water and placed on Whatman GF/B filters preincubated with 2% polyethyleneimine in water. Filters were washed three times with 5 ml of ice-cold  $100\text{ mM}$  KCl,  $1\text{ mM}$  KPipes,  $\text{pH } 7.0$ , solution. The radioactivity remaining with the filters was determined by liquid scintillation counting to obtain the amount of bound [ $^3\text{H}$ ]ryanodine.

**Single Channel Analysis**—Single channel measurements of WT and mutant RyRs were performed in planar lipid bilayers containing phosphatidylethanolamine, phosphatidylserine, and phosphatidylcholine in the ratio of 5:3:2 (25 mg of total phospholipid/ml of *n*-decane) as described previously (13). Crude membrane fractions expressing WT and mutant RyRs were pretreated for 30 min at room temperature with  $1\text{ }\mu\text{M}$  myosin light chain kinase-derived CaM-binding peptide to dissociate endogenous CaM (10). Final peptide concentration was  $<10\text{ nM}$  following the addition of membranes to the cis (cytosolic) chamber of the bilayer apparatus. A strong dependence of single channel activities on *cis*- $\text{Ca}^{2+}$  concentration indicated that the large cytosolic “foot” region faced the cis chamber of the bilayers. The trans (luminal) side of the bilayer was defined as ground. Measurements were made with symmetrical  $0.25\text{ M}$  KCl,  $20\text{ mM}$  KHepes,  $\text{pH } 7.4$ , with  $0.4\text{ }\mu\text{M}$  or  $2\text{ }\mu\text{M}$  free  $\text{Ca}^{2+}$  in the cis chamber. Single channel recordings with WT-RyR1 and chimeras were made in the presence of  $0.4\text{ }\mu\text{M Ca}^{2+}$  and  $1\text{ mM}$  ATP to increase the otherwise very low channel activities. Exogenous CaM was added to the cis solution. Electrical signals were filtered at  $2\text{ kHz}$ , digitized at  $10\text{ kHz}$ , and analyzed as described previously (17).  $P_o$  values in multichannel recordings were calculated using the equation  $P_o = \sum i P_{o,i} / N$ , where  $N$  is the total number of channels, and  $P_{o,i}$  is channel open probability of the *i*th channel.

**Biochemical Assays and Data Analysis**—Free  $\text{Ca}^{2+}$  concentrations were obtained by including in the solutions the appropriate amounts of  $\text{Ca}^{2+}$  and EGTA as determined using the stability constants and computer program published by Shoemaker *et al.* (18). Free  $\text{Ca}^{2+}$  con-

concentrations of  $\geq 1 \mu\text{M}$  were verified with the use of a  $\text{Ca}^{2+}$ -selective electrode. Results are given as mean  $\pm$  S.E. Significance of differences in the data ( $p < 0.05$ ) was determined using Student's  $t$  test.

## RESULTS

To identify the isoform-specific regions involved in CaM modulation, we prepared 10 RyR1- and RyR2-based chimeras and multisite mutants (Fig. 1B) and transiently expressed them in HEK293 cells. All chimeras and mutants showed a  $\text{Ca}^{2+}$  dependence of [ $^3\text{H}$ ]ryanodine binding corresponding to that of WT-RyR1 or WT-RyR2 (19).

**$^{35}\text{S}$ -CaM Binding of RyR2-based Chimeras and Mutants—**The ability of RyR2-based chimeras and mutants to bind CaM was investigated by a centrifugation assay. Three different concentrations of metabolically labeled  $^{35}\text{S}$ -CaM were used at three different  $\text{Ca}^{2+}$  concentrations of 5 mM EGTA ( $\text{Ca}^{2+}$ -free), 0.4  $\mu\text{M}$  free  $\text{Ca}^{2+}$  (a  $\text{Ca}^{2+}$  concentration that results in activation of RyR1 but inhibition of RyR2 by CaM (10)), and 100  $\mu\text{M}$   $\text{Ca}^{2+}$  ( $\text{Ca}^{2+}$ -CaM). The  $B_{\text{max}}$  values of [ $^3\text{H}$ ]ryanodine binding were determined in parallel experiments to determine RyR protein expression levels. Fig. 2 shows that WT-RyR2 bound  $^{35}\text{S}$ -CaM in a concentration-dependent manner. WT-RyR2 bound  $2.0 \pm 0.3$   $^{35}\text{S}$ -CaM per high affinity [ $^3\text{H}$ ]ryanodine-binding site at 200 nM CaM and  $< 10$  nM  $\text{Ca}^{2+}$ , which corresponds to 0.5 CaM per RyR2 subunit because there is only one high affinity [ $^3\text{H}$ ]ryanodine-binding site per RyR2 tetramer. Higher saturating CaM concentrations were not used because these resulted in high background binding levels. The mean numbers of bound  $^{35}\text{S}$ -CaM per RyR2 subunit were 0.6 at 200 nM CaM and 0.4  $\mu\text{M}$   $\text{Ca}^{2+}$  and 0.9 at 75 nM CaM and 100  $\mu\text{M}$   $\text{Ca}^{2+}$  (Fig. 2), which were in good agreement with values reported previously (13). Fig. 2 also shows that all RyR2-based chimeras and mutants (Fig. 1B, left panel) examined in this study bound  $^{35}\text{S}$ -CaM. Some differences in the binding levels were observed; however, none of these were significantly different from WT-RyR2. The expression levels of RyR1-based chimeras and mutants (Fig. 1B, right panel) were too low to determine their CaM binding levels. The  $B_{\text{max}}$  values of [ $^3\text{H}$ ]ryanodine binding were  $\sim 0.1$ – $0.2$  pmol/mg of protein, compared with  $> 0.5$  pmol/mg for RyR2-based chimeras.

**CaM Modulation of RyR2-based Chimeras and Mutants—**Fig. 3 compares the modulation of WT-RyR1 and WT-RyR2 by 50 nM and 1  $\mu\text{M}$  CaM with that of chimera 2-1-2 in the presence of 0.4  $\mu\text{M}$  and 2  $\mu\text{M}$  cytosolic free  $\text{Ca}^{2+}$ . Chimera 2-1-2 has a region of 145 amino acid residues composed of the RyR1 CaMBD and RyR1 N- and C-terminal flanking regions (Fig. 1). 2-1-2 was inhibited by CaM at 2  $\mu\text{M}$   $\text{Ca}^{2+}$ , in accordance with an inhibition of WT-RyR1 and WT-RyR2 by CaM at  $[\text{Ca}^{2+}] > 1 \mu\text{M}$ . At 0.4  $\mu\text{M}$   $\text{Ca}^{2+}$ , CaM had no significant effect on the chimera. 2-1-2 was activated by 50 nM and 1  $\mu\text{M}$  CaM in 6 of 15 and 5 of 13 single channel recordings and inhibited in 5 of 15 and 7 of 13 recordings, respectively. In the remaining channel recordings, CaM was without an effect. The results suggest that regions encompassing and flanking the CaMBD have a role in CaM modulation of the RyRs.

To identify the region that was responsible for loss of a significant effect of calmodulin on 2-1-2 at 0.4  $\mu\text{M}$   $\text{Ca}^{2+}$ , the chimeric region was subdivided into an N-terminal flanking (2-1-2(N)), CaM-binding, and C-terminal flanking (2-1-2(C)) region. As described in a previous study (13), substitution of the four non-identical amino acids in the RyR2 CaM-binding domain (Fig. 1A) with the corresponding amino acids in RyR1 yielded results essentially identical to WT-RyR2. Replacement of the N-terminal flanking region (2-1-2(N)) also did not alter CaM inhibition at 0.4  $\mu\text{M}$  and 2  $\mu\text{M}$   $\text{Ca}^{2+}$  (Fig. 1B). In contrast, exchange of the C-terminal flanking region (2-1-2(C)) eliminated CaM inhibition at 0.4  $\mu\text{M}$   $\text{Ca}^{2+}$  and significant inhibition

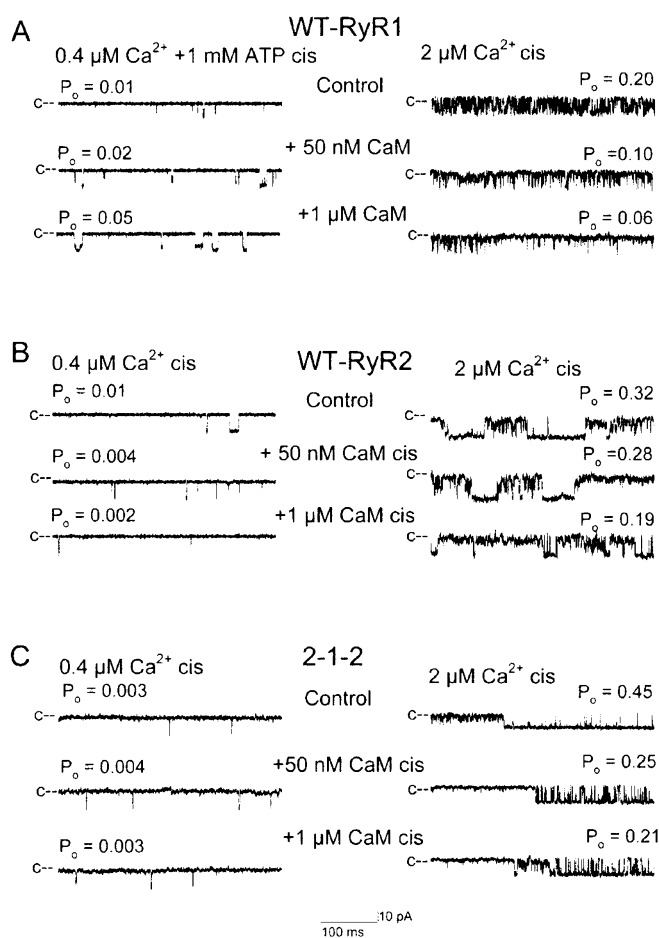


**FIG. 3. Effects of CaM on WT-RyR1, WT-RyR2, and 2-1-2 chimera ion channels.** Membrane fractions prepared from HEK293 cells expressing WT-RyR1 (A), WT-RyR2 (B), or 2-1-2 (C) were fused with a lipid bilayer. Single channel currents were recorded at  $-20$  mV (c, downward deflections from closed level) in symmetric 0.25 M KCl, 20 mM KHepes, pH 7.4, medium with 0.4  $\mu\text{M}$   $\text{Ca}^{2+}$  and 1 mM ATP (WT-RyR1) or 0.4  $\mu\text{M}$   $\text{Ca}^{2+}$  (WT-RyR2 and 2-1-2) (left panels) or 2  $\mu\text{M}$   $\text{Ca}^{2+}$  (right panels) in the cis chamber before (top traces) and after the addition of 50 nM CaM (middle traces) and 1  $\mu\text{M}$  CaM (bottom traces). Data of 4–15 single channel recordings are summarized in Fig. 1B.

at 2  $\mu\text{M}$   $\text{Ca}^{2+}$  by 50 nM (but not by 1  $\mu\text{M}$ ) CaM, notwithstanding that 2-1-2(C) bound  $^{35}\text{S}$ -CaM with an affinity comparable with WT-RyR2.

The N- and C-terminal flanking regions of RyR1 and RyR2 have a sequence identity of 41 and 63%, respectively, compared with 86% for the CaMBD. Secondary structure predictions, using a protein sequence analysis program (bmerc-www.bu.edu/psa/) (20) indicated a nearly indistinguishable helical probability for the RyR1 and RyR2 CaMBDs (Fig. 4A). In contrast, major differences were predicted for both the N-flanking and C-flanking regions. The differences in helical probability of N-terminal flanking regions are caused to a large extent by an RyR2-specific insert (RyR2 aa 3564–3575). We previously showed that an RyR2 mutant lacking this insert bound  $^{35}\text{S}$ -CaM and was inhibited by CaM in a manner essentially identical to WT-RyR2 (13). Therefore, this region does not appear to have a major role in CaM modulation of RyR2. In the C-terminal flanking region, protein sequence analysis predicted several differences in helical probability. In the present study, we address the role of five non-conserved RyR amino acid residues (RyR2 aa 3647 and 3649–3652) that have a profound effect on helical probability. Substitution of these five amino acid residues with those of RyR1 in RyR2 (RyR2–5M) increased helical probability close to that in RyR1 (Fig. 4B). Single chan-

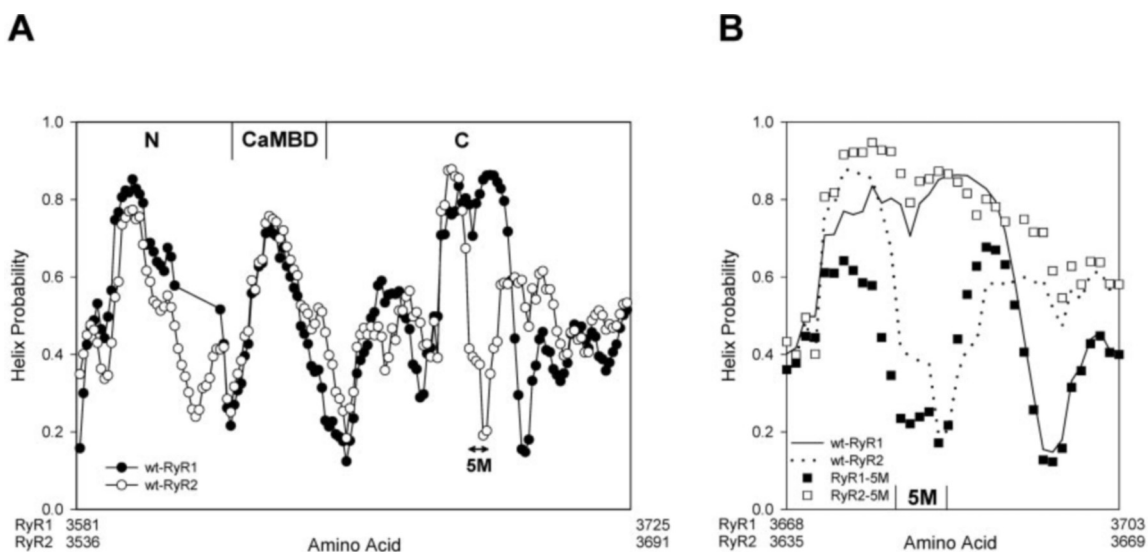


FIG. 4. **Helical probabilities of CaMBD and N- and C-terminal flanking regions.** A, helical probabilities of CaM-binding and flanking regions of RyR1 (filled circle) and RyR2 (open circle) are shown. Each value was calculated from computer program protein sequence analysis (20). N and C, substituted regions in RyR1 and RyR2. B, helical probabilities of RyR1 (solid line), RyR2 (dotted line), RyR1-5M (filled squares), and RyR2-5M (open squares) are shown.

nel measurements showed a loss of inhibition by CaM at  $0.4 \mu\text{M}$   $\text{Ca}^{2+}$  (Figs. 1B and 5A). A role of the five amino acid residues in CaM inhibition of RyR2 was further assessed by substituting the five RyR1 amino acids in 2-1-2 and 2-1-2(C) with those of RyR2. Substitution restored CaM inhibition at  $0.4 \mu\text{M}$   $\text{Ca}^{2+}$  in 2-1-2(C)rev5M but not 2-1-2rev5M (Figs. 1B and 5, B and C). The difference in the ability of the five RyR2 amino acids to restore CaM inhibition was likely the result of the presence of the N-flanking RyR1 region in 2-1-2, because this region contributes to CaM modulation of RyR1 as described below. At  $2 \mu\text{M}$   $\text{Ca}^{2+}$ , RyR2-5M, 2-1-2rev5M, and 2-1-2(C)rev5M were inhibited by CaM (Figs. 1B and 5); however, inhibition was only significant at  $1 \mu\text{M}$  CaM and not  $50 \text{ nM}$  CaM (Fig. 1B), which indicated a decreased efficacy of CaM in modulating the mutant channels.

**CaM Modulation of RyR1-based Chimeras and Mutants**—We also constructed and expressed four RyR1-based reverse chimeras and mutants, 1-2-1, 1-2-1(N), 1-2-1(C), and RyR1-5M. Characterization of RyR1-based chimeras relied on single channel recordings because their expression levels were too low to determine  $^{35}\text{S}$ -CaM binding levels (see above). CaM failed to either activate or inhibit the 1-2-1 chimera (Fig. 1B). Replacement of only the N-terminal flanking region decreased the efficacy of CaM activation at  $0.4 \mu\text{M}$   $\text{Ca}^{2+}$  and, surprisingly, at  $2 \mu\text{M}$   $\text{Ca}^{2+}$  resulted in significant activation of 1-2-1(N) following the addition of  $1 \mu\text{M}$  CaM. In contrast, replacement of the C-terminal region failed to disrupt CaM modulation of 1-2-1(C) at either  $\text{Ca}^{2+}$  concentration. Substitution of the five amino acid residues in RyR1 with those of RyR2 decreased helical probability (Fig. 4B) without affecting CaM activation and inhibition of RyR1-5M (Fig. 1B), which was consistent with the results of 1-2-1(C). Interestingly, at  $0.4 \mu\text{M}$   $\text{Ca}^{2+}$ , CaM activated RyR1-5M to a greater extent than WT-RyR1 (average open probability in the presence of  $1 \mu\text{M}$  CaM was  $1609 \pm 450\%$  ( $n = 4$ ) of control, compared with WT-RyR1 at  $295 \pm 52\%$ ). Taken together, substitution of the N- and C-terminal flanking regions appeared to differentially affect RyR2 and RyR1. Furthermore, substitution of five non-conserved amino acid residues in the C-terminal flanking region resulted in impairment of CaM modulation of the RyR2-5M mutant, without disrupting CaM modulation of the RyR1-5M mutant.

**Role of RyR1 Amino Acid Residues 1975–1999**—Recent tryptic digestion studies and CaM-binding experiments with RyR1

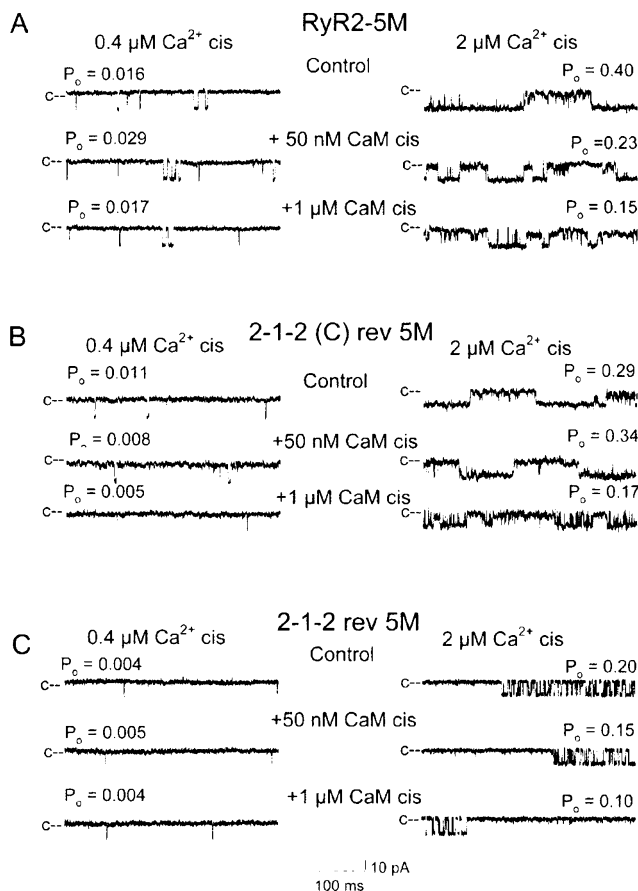
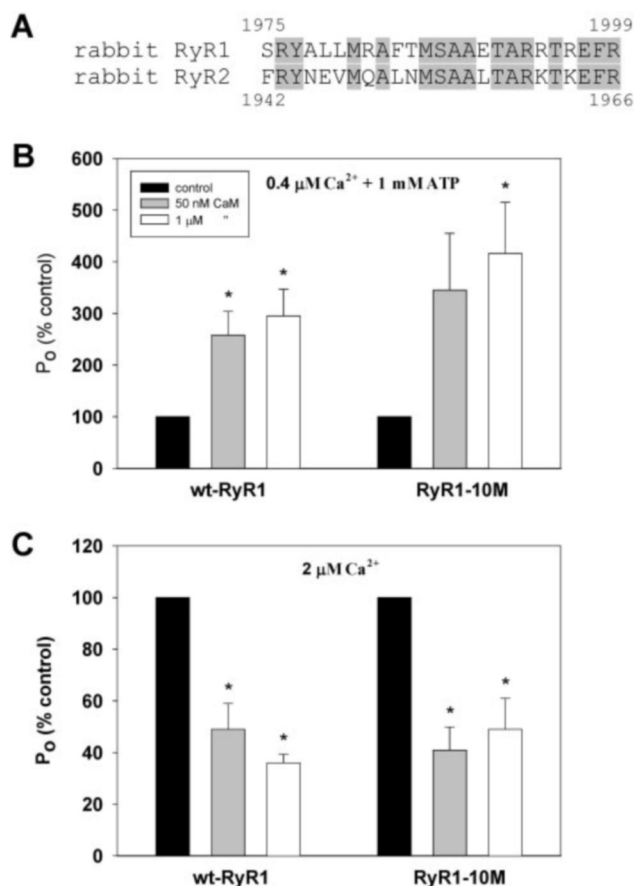


FIG. 5. **Effects of CaM on RyR2-5M, 2-1-2(C)rev5M, and 2-1-2rev5M ion channels.** Single channel currents of RyR2-5M (A), 2-1-2(C)rev5M (B), and 2-1-2rev5M (C) were recorded as in Fig. 3 at  $-20 \text{ mV}$  (c, downward deflections from closed level) in symmetric  $0.25 \text{ M}$  KCl,  $20 \text{ mM}$  KHepes, pH 7.4, medium with  $0.4 \mu\text{M}$   $\text{Ca}^{2+}$  (left panels) or  $2 \mu\text{M}$   $\text{Ca}^{2+}$  (right panels) in the cis chamber before (top traces) and after the addition of  $50 \text{ nM}$  CaM (middle traces) and  $1 \mu\text{M}$  CaM (bottom traces). Data of 4–10 single channel recordings are summarized in Fig. 1B.

peptides indicate that the carboxyl-terminal half of CaM binds to the RyR1 CaM-binding domain, whereas the N-terminal half interacts with RyR1 amino acid residues 1975–1999 (21). There



**FIG. 6. Effects of CaM on WT-RyR1 and RyR1-10M ion channels.** *A*, sequences of putative N-lobe CaM-binding region of rabbit RyR1 sequence (aa 1975–1999) (21) and corresponding rabbit RyR2 (aa 1942–1966) are shown. Sequences and numbering are from References 15 and 16. *B* and *C*, single channel activities of WT-RyR1 and RyR1-10M were determined as described in Fig. 3 in the presence of 0.4  $\mu\text{M Ca}^{2+}$  and 1 mM ATP (*B*) or 2  $\mu\text{M Ca}^{2+}$  (*C*) in the absence (filled bars) or presence of 50 nM (shaded bars) and 1  $\mu\text{M}$  (open bars) CaM. Normalized single channel activities are the mean  $\pm$  S.E. of 4–5 experiments. \*,  $p < 0.05$  compared with control (–CaM).

are 10 non-identical RyR1 and RyR2 amino acid residues in this region. We substituted the 10 aa residues in RyR1 with the corresponding RyR2 residues. The RyR1-10M mutant was activated and inhibited by CaM in single channel (Fig. 6) and [ $^3\text{H}$ ]ryanodine binding (not shown) measurements that were essentially identical to WT-RyR1, which suggests that this region is not responsible for the differential regulation of RyR1 and RyR2 by CaM at  $[\text{Ca}^{2+}] < 1 \mu\text{M}$ .

#### DISCUSSION

Cryomicroscopy studies revealed that the CaM-binding site in the skeletal muscle RyR isoform is at least 10 nm away from the effector site (pore) and that  $\text{Ca}^{2+}$  binding causes an  $\sim 33\text{-\AA}$  shift of the binding site (22). Therefore, long range conformational changes are likely involved in the modulation of RyR activity by CaM. RyR1 and RyR2 each have a single highly conserved CaM-binding region; however, the two RyR isoforms are differentially regulated by CaM, which suggests that isoform-specific regions are involved in transducing the functional effects of CaM. In the present study, we identified one of these regions. Secondary structure predictions indicated a large difference between the helical probability of five non-conserved amino acid residues in the C-terminal region flanking the CaM-binding domain of RyR1 and RyR2. Substitution of the five amino acid residues in RyR2 with those of RyR1 eliminated CaM inhibition at submicromolar  $\text{Ca}^{2+}$  and decreased the effi-

ciency of CaM inhibition at micromolar  $\text{Ca}^{2+}$ . Conversely, substitution of the corresponding RyR2 amino acid residues in RyR1 was without effect on CaM activation and CaM inhibition at  $\text{Ca}^{2+}$  concentrations below and above 1  $\mu\text{M}$ , respectively. Thus, five amino acid residues in the C-terminal region flanking the CaM-binding domain appear to have a specific role in CaM modulation of RyR2.

The RyR2-based chimeras were characterized in  $^{35}\text{S}$ -CaM binding and single channel measurements. Characterization of RyR1-based chimeras relied on single channel measurements because expression levels were too low to obtain reliable  $^{35}\text{S}$ -CaM binding data. Although all RyR2-based constructs bound  $^{35}\text{S}$ -CaM, regardless of whether the constructs contained the RyR1 or RyR2 CaMBD, 2-1-2, 2-1-2(C), and RyR2-5M were unable to convert CaM binding into a functional signal. Interestingly, loss of function was confined to  $[\text{Ca}^{2+}] < 1 \mu\text{M}$  because CaM inhibition was observed at  $[\text{Ca}^{2+}] > 1 \mu\text{M}$ . We also note that the “uncoupled” constructs had a  $\text{K}^+$  conductance and  $\text{Ca}^{2+}$  dependence of [ $^3\text{H}$ ]ryanodine binding comparable with WT-RyR2. The results suggest disruption of the interactions of the CaMBD with protein domains that transduce the functional effects of CaM in RyR2 at  $[\text{Ca}^{2+}] < 1 \mu\text{M}$ .

Ikemoto and Yamamoto (23) have shown that exogenously added RyR1 synthetic peptides alter channel activity by “un-zipping” interdomain interactions in the large RyR1 channel complex. RyR1 mutations giving rise to malignant hyperthermia were suggested to result in elevated channel activities by disrupting interdomain interactions. Zhu *et al.* (24) found that synthetic peptides corresponding to the CaMBD affect RyR1 channel function, which suggested that the exogenously added peptides bound to a region that directly interacts with the CaMBD. Previously, we presented evidence for the importance of three amino acid residues in this interaction in RyR2. Three mutations in the RyR2 CaMBD (W3587A, L3591D, and F3603A) eliminated CaM inhibition at 0.4  $\mu\text{M Ca}^{2+}$ , without an effect on CaM binding (13). The present work extends the previous studies by providing the first clues regarding the identity of regions that transduce the functional effects of CaM in RyR1 and RyR2.

Analysis revealed that substitution of five non-conserved RyR1 amino acid residues in 2-1-2(C) restored CaM inhibition at  $[\text{Ca}^{2+}] < 1 \mu\text{M}$ . On the other hand, substitution of the five RyR1 residues in 2-1-2 did not restore CaM inhibition. Thus, the additional presence of the N-terminal region likely introduced conformational changes that could not be reversed by replacing the five amino acid residues in 2-1-2rev5M. We also tested the role of the two regions flanking the CaMBD in RyR1. Chimera 1-2-1 was not modulated by CaM, in contrast to chimera 2-1-2, which was inhibited at  $[\text{Ca}^{2+}] > 1 \mu\text{M}$ . Further analysis showed that exchange of only the C-terminal flanking region did not eliminate CaM activation and CaM inhibition in the RyR1-based chimera 1-2-1(C), whereas CaM inhibition of 2-1-2(C) was disrupted at  $[\text{Ca}^{2+}] < 1 \mu\text{M}$ . Opposite effects were observed when the N-terminal flanking region was exchanged in RyR1 and RyR2. Replacement of this region did not interfere with CaM inhibition in 2-1-2(N). The efficacy of CaM activation of 1-2-1(N) was reduced at 0.4  $\mu\text{M Ca}^{2+}$  and unexpectedly resulted in CaM activation of 1-2-1(N) at 2  $\mu\text{M Ca}^{2+}$ . Further studies will be required to determine whether the structural elements responsible for activation of 1-2-1(N) lie within the N-terminal flanking region.

Zhang *et al.* (21) suggested that the carboxyl-terminal half of CaM binds to the RyR1 CaM-binding domain, whereas the N-terminal half interacts with RyR1 amino acid residues 1975–1999. We substituted the 10 non-identical amino acid residues in RyR1 with the corresponding RyR2 residues and found that

the mutant was regulated by CaM essentially identical to WT-RyR1, which suggests that this region is not responsible for the differential regulation of RyR1 and RyR2 by CaM at  $[Ca^{2+}] < 1 \mu M$ .

Our data show that the 1-2-1 chimera was not inhibited by CaM, notwithstanding that the chimera contained the RyR2 CaMBD and N- and C-terminal flanking regions. Chimera 2-1-2 was not significantly activated at  $[Ca^{2+}] < 1 \mu M Ca^{2+}$ , despite the presence of the RyR1 CaMBD and flanking regions. These results suggest that additional regions are involved in the CaM modulation of RyR1 and RyR2, as expected considering the large size of the RyRs.

In summary, our structure-function analysis shows that it is possible to use chimeras and multiple site mutants to define the  $Ca^{2+}$ -dependent and isoform-dependent regulation of RyR1 and RyR2 by CaM. The chimeras described here formed channels with a  $Ca^{2+}$  dependence and  $K^+$  conductance comparable with WT-RyRs, which suggests that our structural manipulations did not introduce major global conformational changes, and thus can reveal regions that have a role in the  $Ca^{2+}$ -dependent and isoform-dependent CaM modulation of RyR1 and RyR2. Our work points to one of these regions consisting of five amino acid residues in the C-terminal flanking region of the CaMBD of the RyR2 ion channel.

## REFERENCES

1. Franzini-Armstrong, C., and Protasi, F. (1997) *Physiol. Rev.* **77**, 699–729
2. Fill, M., and Copello, J. A. (2002) *Physiol. Rev.* **82**, 893–922
3. Meissner, G. (2002) *Front. Biosci.* **7**, d2072–2080
4. Rhoads, A. R., and Friedberg, F. (1997) *FASEB J.* **11**, 331–340
5. Saimi, Y., and Kung, C. (2002) *Annu. Rev. Physiol.* **64**, 289–311
6. Balshaw, D. M., Yamaguchi, N., and Meissner, G. (2002) *J. Membr. Biol.* **185**, 1–8
7. Tang, W., Sencer, S., and Hamilton, S. L. (2002) *Front. Biosci.* **7**, d1583–1589
8. Moore, C. P., Rodney, G., Zhang, J. Z., Santacruz-Tolosa, L., Strasburg, G., and Hamilton, S. L. (1999) *Biochemistry* **38**, 8532–8537
9. Fruen, B. R., Bardy, J. M., Byrem, T. M., Strasburg, G. M., and Louis, C. F. (2000) *Am. J. Physiol.* **279**, C724–C733
10. Balshaw, D. M., Xu, L., Yamaguchi, N., Pasek, D. A., and Meissner, G. (2001) *J. Biol. Chem.* **276**, 20144–20153
11. Moore, C. P., Zhang, J. Z., and Hamilton, S. L. (1999) *J. Biol. Chem.* **274**, 36831–36834
12. Yamaguchi, N., Xin, C., and Meissner, G. (2001) *J. Biol. Chem.* **276**, 22579–22585
13. Yamaguchi, N., Xu, L., Pasek, D. A., Evans, K. E., and Meissner, G. (2003) *J. Biol. Chem.* **278**, 23480–23486
14. Gao, L., Tripathy, A., Lu, X., and Meissner, G. (1997) *FEBS Lett.* **412**, 223–226
15. Nakai, J., Imagawa, T., Hakamata, Y., Shigekawa, M., Takeshima, H., and Numa, S. (1990) *FEBS Lett.* **271**, 169–177
16. Takeshima, H., Nishimura, S., Matsumoto, T., Ishida, H., Kangawa, K., Minamino, N., Matsuo, H., Ueda, M., Hanaoka, M., Hirose, T., and Numa, S. (1989) *Nature* **339**, 439–445
17. Gao, L., Balshaw, D., Xu, L., Tripathy, A., Xin, C., and Meissner, G. (2000) *Biophys. J.* **79**, 828–840
18. Schoenmakers, T. J., Visser, G. J., Flick, G., and Theuvsenet, A. P. R. (1992) *BioTechniques* **12**, 870–879
19. Nakai, J., Gao, L., Xu, L., Xin, C., Pasek, D. A., and Meissner, G. (1999) *FEBS Lett.* **459**, 154–158
20. Stultz, C. M., Nambudripad, R., Lathrop, R. H., and White, J. V. (1997) in *Protein Structural Biology in Bio-Medical Research* (Allewell, N., and Woodward, C., eds) Vol. 22B, pp. 447–506, JAI Press, Greenwich, CT
21. Zhang, H., Zhang, J. Z., Danila, C. I., and Hamilton, S. L. (2003) *J. Biol. Chem.* **278**, 8348–8355
22. Samsó, M., and Wagenknecht, T. (2002) *J. Biol. Chem.* **277**, 1349–1353
23. Ikemoto, N., and Yamamoto, T. (2002) *Front. Biosci.* **7**, d671–683
24. Zhu, X., Ghanta, J., Walker, J. W., Allen, P. D., and Valdivia, H. H. (2004) *Cell Calcium* **35**, 165–177